Supramolecular Chemistry
Publication details, including instructions for authors and subscription information:
http://www.informaworld.com/smpp/title~content=t713649759

Molecular motion and phase transitions of clathrate hydrates**

Hiroshi Suga[a]; Takasuke Matsuo[a]; Osamu Yamamuro[a]
[a] Department of Chemistry and Microcalorimetry Research Center, Faculty of Science, Osaka University, Toyonaka, Osaka, Japan

To cite this Article Suga, Hiroshi , Matsuo, Takasuke and Yamamuro, Osamu(1993) 'Molecular motion and phase transitions of clathrate hydrates**', Supramolecular Chemistry, 1: 3, 221 — 233
To link to this Article: DOI: 10.1080/10610279308035165
URL: http://dx.doi.org/10.1080/10610279308035165

SUPRAMOLECULAR CHEMISTRY, Vol. 1, pp. 221–233
Reprints available directly from the publisher
Photocopying permitted by license only

Molecular motion and phase transitions of clathrate hydrates**

HIROSHI SUGA*, TAKASUKE MATSUO and OSAMU YAMAMURO

Department of Chemistry and Microcalorimetry Research Center, Faculty of Science, Osaka University, Toyonaka, Osaka 560, Japan

(Received July 29, 1992)

Heat capacities and complex dielectric permittivities of three clathrate hydrates of type II, encaging tetrahydrofuran (THF), acetone (Ac), and trimethylene oxide (TMO), were measured at low temperatures. The heat capacity measurement was done in the temperature range 13–300 K by using an adiabatic calorimeter with a built-in cryorefrigerator. The permittivities were measured in the temperature range 20–260 K and in the frequency range 20 Hz–1 MHz. For pure samples, with a glass transition due to freezing out of water, reorientational motion of the host lattice was observed calorimetrically at 85 K for THF and at 90 K for Ac hydrates, respectively. Spontaneous temperature drift rates of the calorimetric cell were measured under adiabatic conditions to derive the characteristic time for enthalpy relaxation. The enthalpy relaxation times thus derived were well correlated in an Arrhenius plot with the dielectric relaxation times derived from the dielectric relaxation of orientation polarization. The situation is the same as hexagonal ice which has a similar four co-ordinated hydrogen-bonded network.

Each sample was doped with KOH in a mole fraction of 1.8×10^{-4} to water. The dopant was found to shorten dramatically the relaxation time for water reorientation in hexagonal ice. Actually, the KOH-doped clathrate hydrate exhibited a first-order phase transition with a considerable amount of entropy change. The temperature and entropy of the transitions were 61.9 K and 40.1 J K^{-1} mol^{-1} for $THF \cdot 17H_2O$, 46.6 K and 42.2 J K^{-1} mol^{-1} for $Ac \cdot 17H_2O$ and 34.5 K and 40.1 J K^{-1} mol^{-1} for $TMO \cdot 17H_2O$, respectively. If the entropy of transition is referred to 1 mole of water, the values 2.3–2.4 J K^{-1} $(H_2O\text{–mol})^{-1}$ are similar in magnitude to that of KOH-doped ice.

The temperature region in which the dielectric relaxation due to the water dipoles occurs was lowered by more than 100 K by the KOH doping. The relaxation time was shortened by factors of 10^{10}–10^{12} at 70 K and the activation energy was reduced to roughly one-third of that for the pure specimen. Thus the dopant accelerated dramatically the water motion to release the immobilized frozen-in state at low temperatures and to induce their ordering transition as an intrinsic equilibrium property of the clathrate hydrate. The dielectric relaxation due to the guest molecule was found to disappear in the low temperature phase of the THF and Ac hydrates, indicating that both the host and guest molecules ordered concomitantly at the transition. For the TMO hydrate, for which the effective van der Waals diameter was the smallest of the three, the dielectric dispersion persisted below the transition temperature. This indicated that the ordering of the host lattice could not produce an electric field strong enough to align the guest molecule of such a small size. The distribution of relaxation times for the water motion became broad as the temperature was lowered. An interesting time-dependence of the static dielectric permittivity of pure THF hydrate was observed at approximately 87 K. This reflected the relaxation behaviour of the water dipoles which affected the orientation polarization of the guest molecules through host–guest interaction.

Excess heat capacities associated with the fusion (single peak for congruent melting of THF, and double peaks for incongruent types of Ac and TMO) were analysed to determine the enthalpy of fusion. The value for Ac and the literature values of the enthalpies of fusion and vaporization for component crystals, and of the enthalpy of mixing for the binary system, were combined to derive the enthalpy of enclathration of acetone into an ice lattice to form the clathrate hydrate.

INTRODUCTION

The term 'gas hydrate' has long been applied to the solids that are produced by the dissolution of many gases into water at sub-ambient temperatures. The study goes back to the 19th century when Davy found

* To whom correspondence should be addressed. ** Contribution No. 67 from the Microcalorimetry Research Center.

a crystalline substance in an aqueous solution of chlorine. Nowadays, these hydrates are regarded as one kind of clathrate compound, the concept of which as introduced by Powell[1] for the structural combinations of two substances in which strong mutual binding of molecules of one sort makes possible a firm enclosure of the other. Many of the clathrate hydrates from type I and II lattices, as defined by MacMillan and Jeffrey.[2] The unit cell of the type II clathrate hydrate, with which the present study is concerned primarily, is composed of 16 pentagonal dodecahedral and eight hexakaidecahedral cages formed by 136 water molecules connected to each other through hydrogen bonds. Thus the host lattice has a three-dimensional hydrogen-bonded network similar to many polymorphs of ice. Most of the guest molecules in the type II hydrates are encaged only in the larger cages, so that the stoichiometric formula for the full occupation of a guest molecule M is $M{\cdot}17H_2O$.

One of the fascinating problems in the clathrate hydrates is that there are two kinds of orientational disorder for both of the host and guest molecules. This double disorder is a special feature of the clathrate hydrates and their ordering phenomena have been one of the active subjects in the research of this field. For the clathrate hydrates encaging dipolar guest species, two kinds of dielectric dispersion are exhibited.[3] The one occurring at 160–180 K for 1 kHz is ascribed to the freezing-out of reorientational motion of the water molecules and resembles that of ordinary ice. The static dielectric permittivity is 70–90 at 140 K and increases in the form A/T with decreasing temperature, regardless of the type of guest molecule. The static permittivity falls down by the dielectric relaxation of the water dipole to $\varepsilon_{\infty 1}$, which is composed of two contributions; orientation polarization of the guest molecule and electronic polarization of the whole system. The symbols $\varepsilon_{\infty 1}$, and ε_{02} are used synonymously for this reason, where the suffixes 1 and 2 refer to water and guest molecules, respectively. The other dispersion occurring at cryogenic temperatures is due to the freezing-out of the guest dipoles, indicating a high mobility of the guest species inside the almost spherical cavity. Most probably, slow dynamics of the water molecules at low temperatures hinders the host lattice in realizing their ordered structures that satisfy the third law of thermodynamics. Freezing-in of the host water molecules with respect to their orientations would not produce a crystalline field which forces the guest molecule to align along a preferred orientation at the lowest temperatures. Both of the host and guest molecules are frozen in a disordered orientation, and the corresponding entropy cannot be fully removed.

In this paper, thermodynamic and dielectric properties of the clathrate hydrates encaging tetrahydrofuran (THF), acetone (Ac), and trimethylene oxide (TMO) are reviewed. For pure specimens, a glass transition due to freezing of the host water was observed calorimetrically, and the rate of enthalpy relaxation was analysed to derive the kinetic parameters governing the relaxation process. For KOH-doped specimens, a first-order phase transition was observed due to dramatic enhancement effects of the dopant on the mobility of water molecules. The associated entropy changes were compared with each other and with that of doped ice to clarify the mechanism of the ordering process. Dielectric permittivity data were analysed to derive the dielectric relaxation time as well as the distribution of the relaxation times as a function of temperature for both the host and guest molecules. Preliminary results of the analysis of neutron diffraction patterns for fully deuterated THF hydrate are briefly described.

EXPERIMENTAL SECTION

Preparation of clathrate hydrates

Commercial reagent grade THF, Ac and TMO were purified by fractional distillation with a high-quality rectifier and by dehydration with molecular sieve in vacuo, respectively. No trace of organic impurity was detected by gas chromatography (Perkin–Elmer F21). Water was purified by distillation followed by deionization. Conductance of the purified water was approximately 60 nS m^{-1}.

Each sample solution was prepared gravimetrically by mixing the guest liquid with water under helium. A slightly guest-rich composition from the ideal one ($M{\cdot}17H_2O$) was chosen to avoid the effect of dielectric relaxation due to excess ice. For doped samples, aqueous solutions of KOH (0.01 mol dm^{-3}), corresponding to a mole fraction of 1.8×10^{-4} KOH against H_2O, were used in place of purified water. After a careful deaeration, the sample solution was loaded into respective sample cells for calorimetric and dielectric measurements either by vacuum distillation or by an injector under helium.

The clathrate hydrates of Ac[4] and TMO[5] exhibit incongruent melting behaviour, in contrast to congruent melting of the THF[6] hydrates. Formation of a sample crystal for the former two was carefully done by annealing the sample solution at several temperatures below its peritectic point until the exothermic effect due to homogenization of the composition ceased almost completely. The extent of hydrate formation was confirmed by measuring the enthalpy change associated with the eutectic melting which exists below the corresponding peritectic point.

Calorimetric measurement

A low-temperature adiabatic calorimeter with a built-in cryo-refrigerator[7] was used. Low temperatures, down to 20 K, were available without use of any coolants. The calorimeter proved to be useful for a long annealing experiment at cryogenic temperatures as performed in this study. The heat capacity measurement was carried out in the temperature range 11–300 K; temperatures below 20 K were obtained by pumping liquefied hydrogen condensed in a coolant tank of the cryostat. The calorimetric cell was made of gold-plated copper with fins for better heat distribution. A small amount of helium gas was introduced inside the cell for rapid thermal equilibration. Measurement was made by an intermittent heating mode, so that the measuring operation was repetitious of the energizing period and equilibration period. The accuracy of the heat capacity data was 1% below 20 K, 0.3% between 10 and 50 K, and 0.1% above 50 K.

Dielectric measurement

Complex dielectric permittivity was measured by an LCR meter (Yokogawa Hewlett Packard 4284A) for the frequency range 100 Hz–1 MHz and a capacitance bridge (General Radio 1615A) for 20–100 Hz. The cryostat used in this study is described elsewhere.[8] Stability of the cell temperature was within 0.02 K, and the accuracy of the temperature measurement by use of a chromel–constantan thermocouple was ± 0.1 K. The cell constant and the floating capacitance, calibrated against vacuum and purified benzene, were 0.842 pF and 0.0132 pF, respectively.

Neutron diffraction

A neutron diffraction experiment was carried out on the doped THF hydrate using a high-resolution powder diffractometer at the pulse neutron source ISIS of the Rutherford Appleton laboratory. The data were collected in the time-of-flight range of 30–190 μs, corresponding to a d-spacing range of 0.6–4.0 Å, with a resolution ($\Delta d/d$) of 0.05%. The experiment was performed under the collaboration of W.I.F. David and R.M. Ibberson as one subject in our mini Anglo–Japan Joint Research Projects in order to examine dynamic and static aspects of both the host and guest molecules.

RESULTS

Heat capacity

Figure 1 shows the molar heat capacity of the pure Ac hydrate[9] in the low temperature region. No phase transition was observed across the whole temperature range but a glass transition with a heat capacity jump of 9.7 J K^{-1} mol^{-1} was found at approximately 90 K, as is shown clearly in the inset to Figure 1. Spontaneous temperature-drift rates, due to an irreversible enthalpy relaxation from a frozen-in that was disordered to the equilibrium state, are plotted in Figure 2 as a function of temperature. The rates were observed during each equilibration period at 10 min after each energy input. In the continously cooled sample, a series of exothermic followed by endothermic drifts appeared in the temperature range 70–95 K. In the sample annealed at 80 K for 30 h, only endothermic

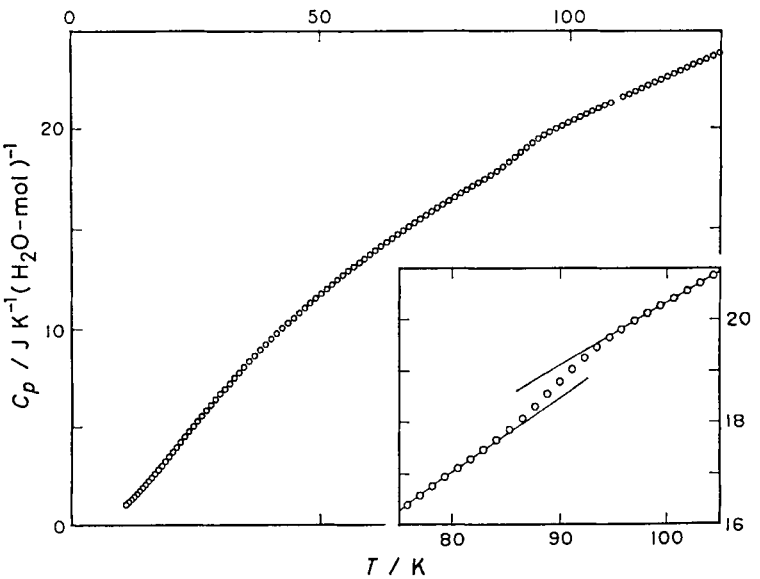

Figure 1 Molar heat capacity of pure crystalline Ac·17H_2O at low temperature.

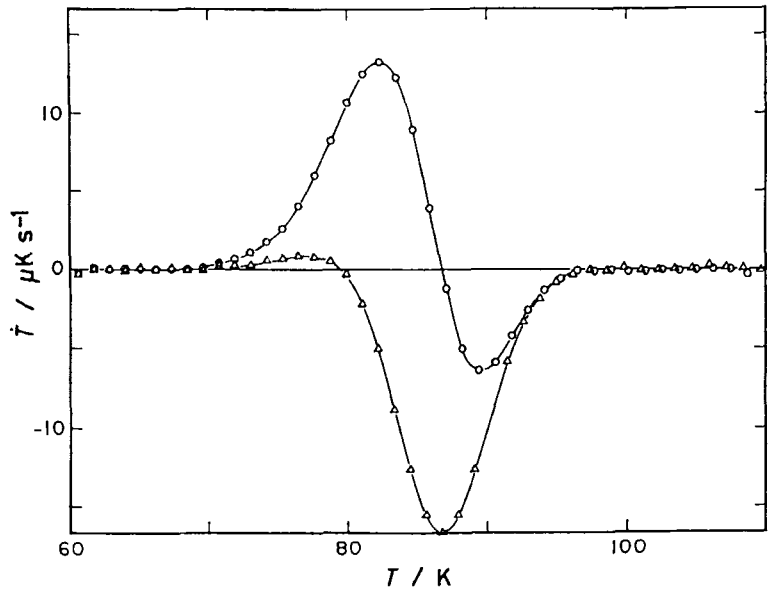

Figure 2 Spontaneous temerature drift rates of pure Ac·17H_2O in the glass transition region. ○: cooled at 0.04 Ks^{-1}, △: annealed at 80 K for 30 h.

drifts appeared, starting from the annealing temperature. This type of relaxational heat-capacity anomaly is one of the characteristic features of the glass transition. The spontaneous temperature drifts are due to recovery of the equilibrium configurational enthalpy which is related to molecular motion frozen at the glass transition.

In most of the frozen-in non-equilibrium systems, typically observed in glasses produced by rapid cooling of liquids,[10] the relaxation rate of any physical property $\phi(t)$ can be described by the Kohlrausch–Williams–Watts function:[11]

$$\phi(t) = \phi(0)\exp[-(t/\tau)^{\beta}], \qquad (1)$$

where $\phi(t)$ and $\phi(0)$ are departures of the physical property from the equilibrium value at time t and 0, τ is the relaxation time, and β the non-exponential parameter. For $\beta = 1$, the equation becomes the Debye-type relaxation function with a single time constant τ. The physical quantity relevant to the present experiment is the excess configurational enthalpy H_c^{ex} beyond the equilibrium enthalpy. For calorimetric measurement under adiabatic conditions, the equation can be modified as follows[12] to reproduce the actual temperature change observed during a long equilibration period:

$$T(t) = A + Bt - C\exp[-(t/\tau)^{\beta}] \qquad (2)$$

Here, $T(t)$ is the calorimetric temperature at time t, $A-C$ the initial temperature, B the constant drift rate due to residual heat leakage, C the amplitude of the relaxation, τ the relaxation time, and β the stretched exponential parameter. This equation can be applied to the variation of calorimetric temperature observed as a function of time under adiabatic conditions.

A similar glass transition was observed in the pure THF hydrate at approximately 85 K.[13] The enthalpy relaxation times derived from the analysis of the calorimetric temperature could be well correlated with the dielectric relaxation time data[4,14,15] in an Arrhenius plot for both of the clathrate hydrates. This means that the glass transition is associated with the freezing-out of water reorientational motion in the host lattice. The situation is similar to that of hexagonal ice.[16] The reorientational motion of water molecule slows down progressively as the temperature is lowered, and the crystal is brought into a non-equilibrium disordered state before it reaches a hypothetical ordering transition. The derived values of β are in the range 0.4–0.8 for both hydrates and are close to those for many glass-forming liquids[17] below their glass transitions. Since the guest molecules are known to freeze at cryogenic temperatures, the clathrate hydrates provide a new category of glassy crystals[18] in which the molecules are frozen-in disordered with respect to their orientations, keeping the translational periodicity with respect to their centres of mass for both the host and guest species.

Dopant-induced phase transition

In order to observe a possible ordering process of the host water molecules as an intrinsic property of the clathrate hydrate, it is necessary to accelerate the water

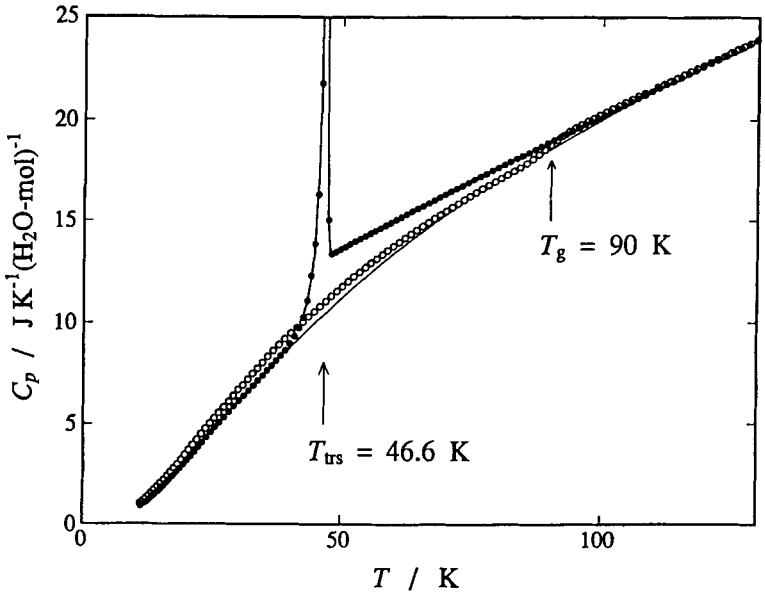

Figure 3 Molar heat capacities of pure (○), and KOH-doped (●), crystalline Ac·17H_2O.

reorientational motion so that the molecules realize an ordered state with respect to their orientations within a reasonable experimental time. This was successfully done by doping each sample with a small amount of KOH. The acceleration effect of KOH on the water reorientational motion was first observed in hexagonal ice;[19] a first-order phase transition was induced in KOH-doped ice at 72 K with a considerable amount of associated entropy change which was a substantial fraction of the residual entropy.

Figure 3 shows the heat capacity of the KOH-doped Ac·16.97H_2O sample.[20] The data are referred to 1 mole of water. The crystal underwent a first-order phase transition at 46.6 K with a significant short-range effect at the high temperature side. The mole fraction x of KOH to H_2O was 1.8×10^{-4}. The associated entropy change was 42.1 J K^{-1} mol^{-1} or 2.48 J K^{-1} (H_2O-mol)$^{-1}$. The latter quantity is close to that of hexagonal ice. For the KOH-doped clathrate hydrates of THF[21] and TMO,[22] the corresponding transitions occurred at 61.9 K and 34.5 K, respectively. Thus the dopant was found to be highly effective in shortening the relaxation time for the water reorientational motion, as in the case of hexagonal ice. The excess heat capacity and entropy associated with the first-order transition are shown in Figure 4 as a function of temperature for the three KOH-doped samples. In each case, the high-temperature asymptotic entropy value is approximately 2.4 J K^{-1} (H_2O-mol)$^{-1}$. The excess entropy is composed of two contributions; a discontinuous jump at the transition temperature and a continuously increasing part extending above the temperature. It is interesting that the relative magnitude depends on the transition temperature. The lower the transition temperature is, the higher the short-range ordering effect is. For TMO clathrate hydrate, the discontinuous increase at the transition contributes merely one-third of the total entropy change.

Dielectric relaxation due to water dipoles

Figures 5 and 6 draw the dielectric permittivity of the KOH-doped Ac hydrate[23] in the high and low temperature regions, respectively. The upper and lower graphs in each Figure correspond to the real (ε') and imaginary (ε'') parts of the permittivity. The vertical broken line gives the transition temperature determined calorimetrically. For pure specimens,[4] the dielectric relaxation due to water dipoles was observed in the temperature range 100–200 K. The peak temperature of ε'' measured at 1 kHz was 166 K. For the doped sample examined, the dielectric relaxation due to water molecules shifted to lower temperatures by more than 100 K. This result gives more evidence that the reorientational motion of water molecules in the host cage was accelerated dramatically by the doping.[24]

The dielectric relaxation was found to disappear completely below the transition temperature. No anomalous behaviour was observed at around 30 K where the second dielectric relaxation due to acetone dipoles was found in the pure samples.[4] This result means that both of the host and guest molecules are fully ordered at the transition temperature. Essentially the same result was obtained for the doped THF hydrate.[25] For the doped TMO hydrate, dielectric

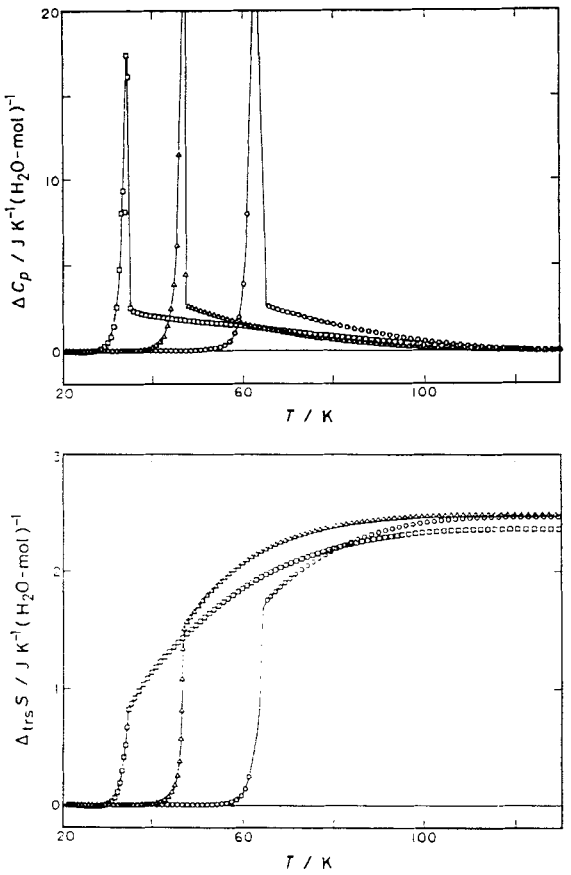

Figure 4 Molar excess heat capacities (upper) and excess entropies of KOH-doped structure II clathrate hydrates of THF (○), Ac (△), and TMO (□).

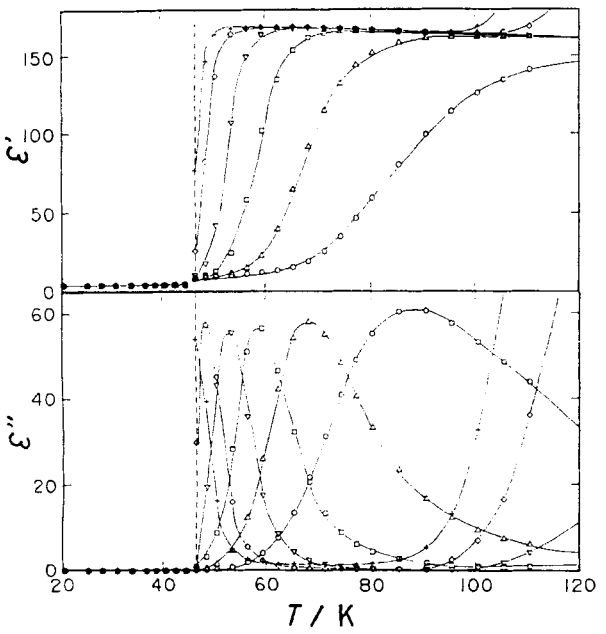

Figure 5 Temperature dependence of real (upper) and imaginary (lower) parts of the dielectric permittivity of KOH-doped acetone hydrate in the high temperature region. ○: 1 MHz, △: 100 kHz, □: 10 kHz, ▽: 1 kHz, ○: 100 Hz, +: 20 Hz.

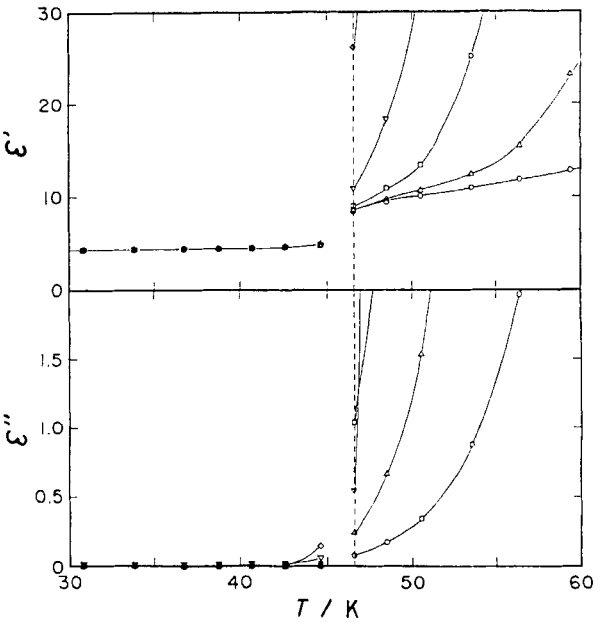

Figure 6 Temperature dependence of real (upper) and imaginary (lower) parts of the dielectric permittivity of KOD-doped acetone hydrate in the low temperature region. ○: 1 MHz, △: 1 kHz, □: 10 kHz, ▽: 1 kHz, ○: 100 Hz, +: 20 Hz.

relaxation due to water reorientation similarly occurred in the temperature region of approximately 100 K lower than that of the pure sample. At the transition temperature, however, no discontinuous change of dielectric permittivity was observed. This is because the reorientational motion is too sluggish in the doped TMO hydrate to be detected by the lowest frequency used in this experiment. One unexpected observation was that the dielectric relaxation due to the TMO dipole was observed at below the transition temperature, in contrast to the clathrate hydrates of THF and Ac. This will be discussed later.

Figure 7 depicts the complex dielectric permittivity of the doped Ac hydrate for water polarization. This Figure is typical of all the structure II hydrates examined here. The results can be compared with those of pure hydrates.[4] These loci are represented as circular arcs with centres lying below the axis of the abscissas, as given by the Cole–Cole equation:

$$\varepsilon^* = \varepsilon_{\infty 1} + \frac{\varepsilon_0 - \varepsilon_{\infty 1}}{1 + (i\omega\tau)^{1-\alpha}} \qquad (3)$$

for the complex permittivity in terms of the limiting values of permittivity ε_0 and $\varepsilon_{\infty 1}$, reached at low and high frequencies, the effective relaxation time τ, and the distribution parameter α. For the pure Ac hydrate, the reported value of ε_0 is 70 at 236 K and 83 at 187 K. For the doped sample, ε_0 increases to 167 at 68.3 K. At the same time, the distribution parameter α increases progressively as the temperature is lowered.

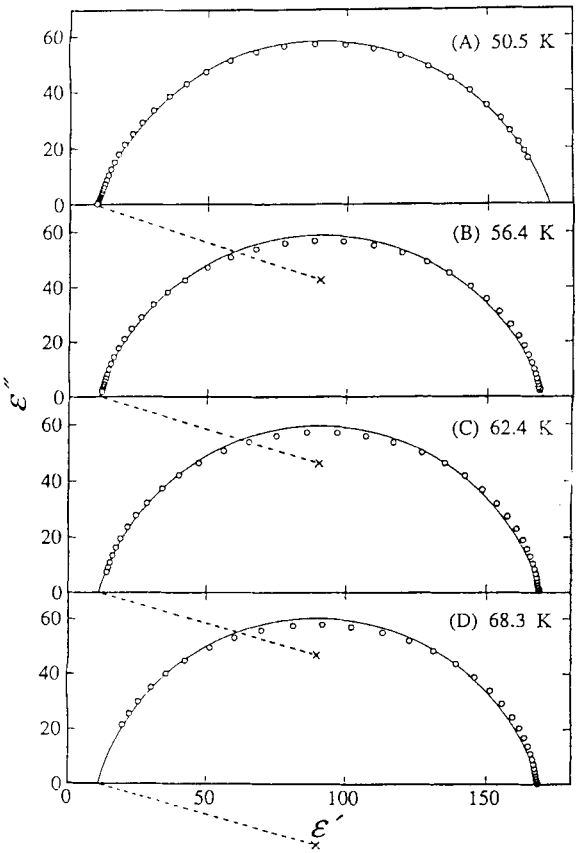

Figure 7 Complex permittivity plots associated with the dielectric relaxation due to water reorientation in KOD-doped acetone hydrate.

The effective relaxation time τ for the water reorientational motion can be calculated from the frequency which gives the maximum value of ε'' with the following equation:

$$\tau = (2\pi f_{max})^{-1} \quad (4)$$

The relaxation times thus calculated for the three doped hydrates are plotted in Figure 8 against reciprocal temperature. As shown by the straight lines in the Figure, all the data can be fitted well to Arrhenius equation:

$$\tau = \tau_0 \exp(-E_a/RT) \quad (5)$$

The activation energy E_a obtained by least-squares fitting is 7.4 kJ mol^{-1} for THF, 8.5 kJ mol^{-1} for Ac and 9.0 kJ mol^{-1} for TMO hydrates, respectively. These three values can be compared with those for pure hydrates; 31.0 kJ mol^{-1} for THF, 27.2 kJ mol^{-1} for Ac and 29.3 for TMO. The relaxation time itself is reduced dramatically by the doping. The reduction factor evaluated at, say 70 K, by extrapolating some data to this temperature is roughly 10^{-10} for THF and 10^{-12} for Ac hydrates, respectively.[26] Thus the dopant, even a minute amount, shortens dramatically the relaxation time and diminishes the activation energy for the water reorientational process in the lattice of the clathrate hydrates.

As is well known, reorientation of the water dipole in a fully four co-ordinated hydrogen-bonded network is not possible without the co-operative movement of a neighbouring water dipoles.[27] The most successful mechanism proposed to account for the large orientation polarization due to water molecules in ice and related hydrogen-bonded systems is that of Bjerrum,[28] who postulated a pair of orientational defect bonds produced by occasional misorientation of a water molecule. The defect bonds are composed of a D bond possessing two protons and an L bond possessing none in the relevant two hydrogen bonds. The process of diffusion of these defects affects the orientation polarization through the configurational change that occurs along the diffusion path of the defects. The catalytic action continues until each of them is annihilated by occasional encounter with a defect of the opposite kind. Again, thermal fluctuation produces another pair of the orientational defects at a different site and continues to contribute to the orientation polarization.

In pure ice, the concentration of these defects is believed to be of the order of 10^{-7} mole fraction at 260 K, and to decrease exponentially as the temperature is lowered. A hydroxide ion of KOH can replace one water molecule in the lattice and create an orientational L defect with negative charge. Thus the dopant acts to introduce artificial L defects into the lattice even in

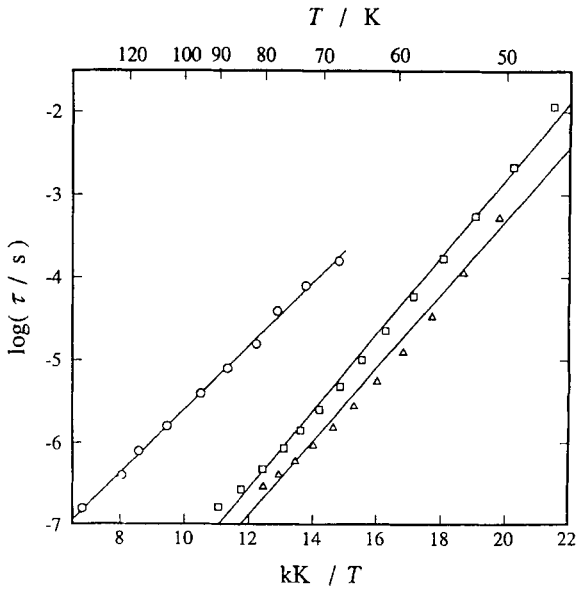

Figure 8 Temperature dependence of the relaxation times of water reorientation in KOH-doped structure II hydrates of THF (○), acetone (△), and TMO (□).

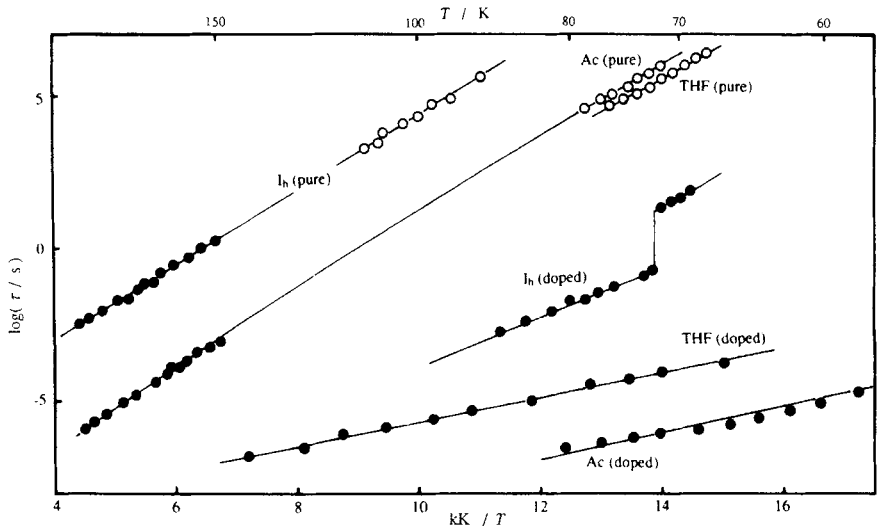

Figure 9 Temperature dependence of the relaxation times of water reorientation in pure and KOH-doped ices and structure II clathrate hydrates obtained calorimetrically and dielectrically.

a mole fraction of 10^{-4}. This concentration far exceeds that of the intrinsic defects and can be kept to the same level of concentration irrespective of temperature. The associated negative charge polarizes the surrounding hydrogen bonds and easily attracts the neighbouring proton, resulting in an enhanced diffusional process of the defects with less activation energy. This picture explains some facets of the dramatic acceleration effect of KOH dopant on water reorientational motion in ice and clathrate hydrates which are constructed by similar hydrogen-bonded networks. Figure 9 summarizes the relaxation time data of ice and clathrate hydrates obtained calorimetrically and dielectrically. The data are given in an Arrhenius form and the data for TMO hydrate are omitted for clarity. It is interesting to note that both the enthalpy and dielectric relaxation times lie on the same straight line over a wide range of time-scale extending over 12 orders of magnitude. In view of the high thermal stability and temperature resolution, the adiabatic calorimeter works as an ultra-low frequency spectrometer[29] and produces static as well as dynamic data which are complementary to the dielectric data.

Figure 10 shows the temperature dependence of the parameter α determined for the three clathrate hydrates in both pure and doped states. The acceleration effect of the dopant on water reorientational motion made it possible to obtain the data over an unusually wide range of temperature, 50–240 K. The distribution of relaxation times becomes wider as the temperature is lowered. This is considered to be associated with the rate of guest reorientational motion, which is little affected by the dopant and is suppressed progressively with decreasing temperature. The field produced at the site of the water molecule by fluctuating guest molecules may be well averaged and more isotropic with increasing temperature. The situation brings about a more uniform reorientational process of the water molecules at higher temperatures, resulting in smaller value of α.

Dielectric relaxation due to TMO dipole

As stated in the previous section, the dielectric relaxation due to the guest dipole was observed only in the TMO hydrate below the transition temperature. This means that the guest TMO molecules are still orientationally disordered in the environment of an ordered host lattice. It is reasonable to consider that a part of the high temperature phase persisted unchanged down to the lowest temperature. Long annealing times were given to each sample at several temperatures below its transition temperature in order to complete the transformation. For the doped TMO hydrate, the sample was annealed at 31.9 K for 3 h, 30.1 K for 7.5 h and at 28.1 K for 4.5 h prior to the measurement. The sample thus stabilized showed a constant dielectric permittivity which is invariant with time.

It was imagined originally that the ordering of the host water molecules produced a strong electric field at the guest site which forced the guest molecules to align along a preferred orientation. We must however seek another explanation for the different behaviour of the motion of guest species below the transition temperature. One important factor to be taken into consideration is that TMO molecules have the smallest van der Waals diameters (550 pm compared with 590

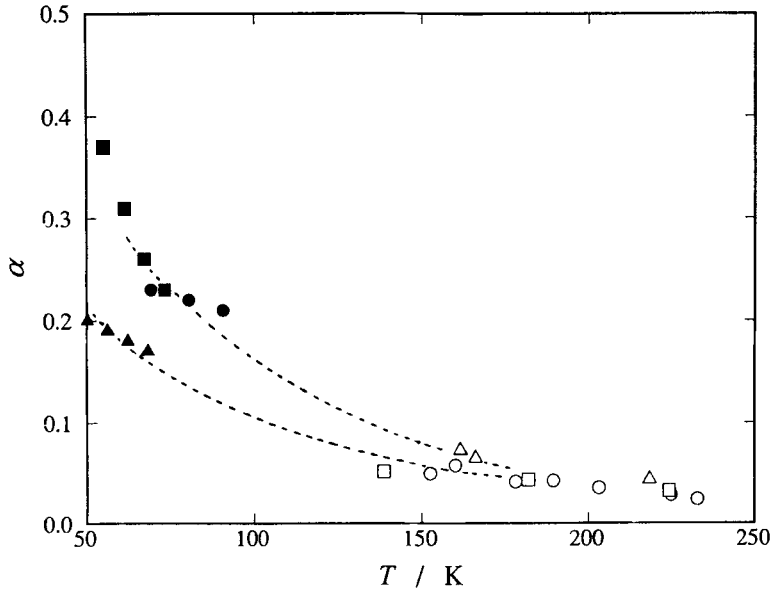

Figure 10 Temperature dependence of the α parameters associated with dielectric relaxations due to water reorientation in KOH-doped hydrates of THF (●), acetone (▲), and TMO (■), and in pure hydrates of THF (○), acetone (△), and TMO (□).

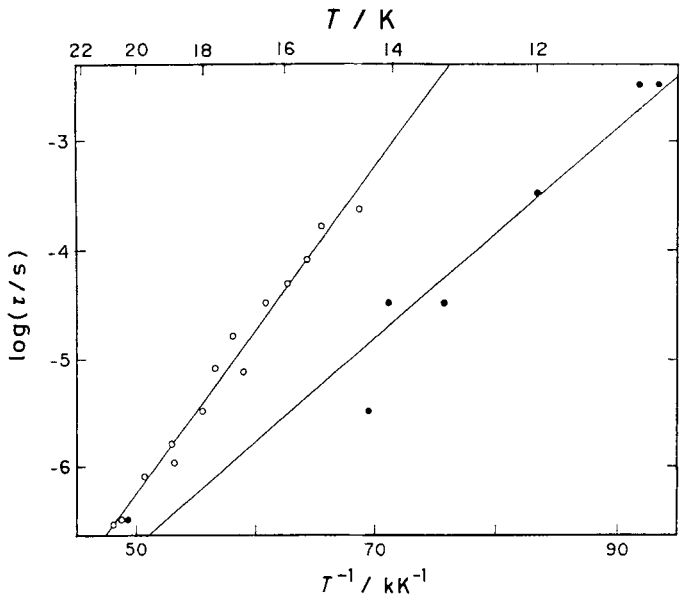

Figure 11 Temperature dependence of the relaxation times for TMO reorientation in structure II TMO hydrates. ○: KOD-doped, ●: pure.

pm for THF and 630 pm for Ac). The small size of the guest molecule inside the same size of cavity will result in greater reorientational mobility of the TMO molecule in the low temperature phase. Also we have no reason to expect that all the low-temperature phases have the same ordered structure. Different extents of possible deformations of the cage, depending on the size of guest molecule, will be another factor to take into account.

Figure 11 shows an Arrhenius plot of the relaxation times for TMO reorientational motion in the low-temperature phase of the doped sample. The relaxation times for the pure sample are also plotted (filled circles). The latter data correspond to those for the frozen-in high-temperature disordered phase. The temperature dependence of the relaxation time for the doped sample is clearly different from that for the pure sample. The activation energy obtained by fitting the data to the Arrhenius equation was 2.89 kJ mol^{-1} for the doped and 1.84 kJ mol^{-1} for the pure hydrates,

respectively. This means that TMO molecules in the cage in the low-temperature phase are bound more tightly than in the frozen-in disordered state. A possible deformation of the cage and the electric field produced inside the cage, which occur at the phase transition, will be involved in an increased anisotropy of the potential field for the guest reorientational motion.

In both samples, the distribution of the relaxation times for the TMO reorientation is much broader than that for the water reorientation. In the doped sample, the value α is 0.42 at 18.8 K, 0.52 at 17.0 K, 0.61 at 16.0 K, and 0.67 at 14.6 K. These values are a little lower than those in the pure sample. In the pure hydrate, the origin of the wide distribution of the relaxation times was considered to be due to the fact that the cage-forming water molecules are frozen-in disordered below the glass transition temperature. It is also difficult to understand the large negative temperature dependence of α observed in both samples irrespective of the extent of order of the host cage. We imagine that the TMO reorientation in the low temperature region is affected significantly by the guest–guest interaction, which is a minor effect compared with the overwhelming guest–host interaction at high temperatures.

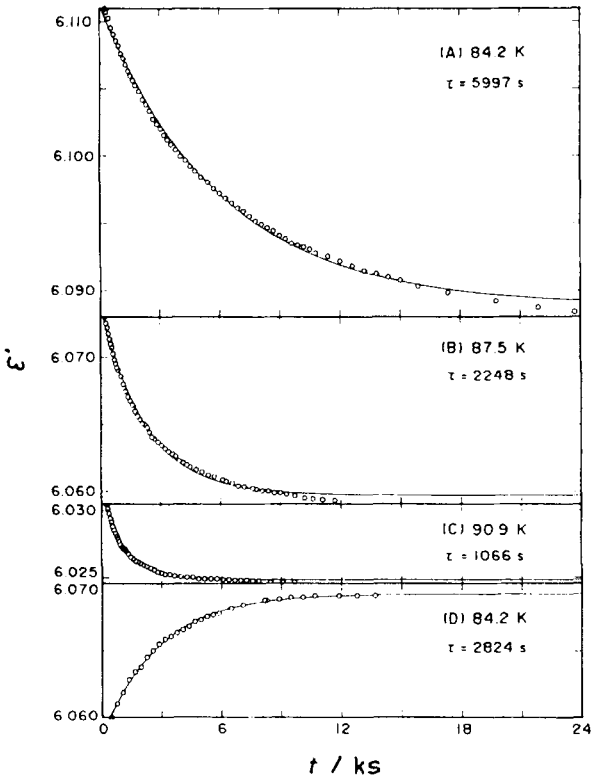

Figure 12 Time dependence of ε' measured at 100 kHz of pure THF hydrate kept at several temperatures at around T_g. The sample was cooled rapidly from 100 K down to 84.2 K (curve A), 87.5 K (B), 90.1 K (C), and warmed to 84.2 K (D) after annealing at 78 K for 48 h.

Relaxation of static permittivity

The glass transition associated with the freezing out of the water reorientational motion in the host cage can be studied dielectrically. This is because the relaxation process should affect to some extent the high-frequency limiting value $\varepsilon_{\infty 1}$ $(= \varepsilon_{02})$ of the permittivity around the glass transition region. This expectation was hinted at by the previous dielectric measurement reported by Garg *et al.*[30] The ε_{02} $(= \varepsilon_{\infty 1})$ value, corresponding to the static dielectric permittivity due to guest molecule, follows approximately the Curie law at high temperatures. This behaviour is in accord with the idea that the guest molecules effectively undergo isotropic reiorientation at high temperatures. At lower temperatures ε_{02} ceases to increase as $1/T$ increases, it passes through a broad flat maximum, and finally falls down to $\varepsilon_{\infty 2}$ by the dielectric dispersion occurring at the cryogenic temperatures. Departure from Curie behaviour was found in the present experiment to occur in the temperature region where the short-range ordering effect of the water molecules develops appreciably. This observation suggests real existence of correlations between the dielectric behaviour of the host and guest molecules. This conjecture has proved to be the case.

Figure 12 shows the time dependence of ε' measured at 100 kHz of the pure THF hydrate kept at several temperatures at around T_g.[25] The sample was cooled rapidly from 100 K down to 84.2 K (curve A), 87.5 K (B), 90.1 K (C), and warmed rapidly to 84.2 K (D) after annealing at 78 K for 48 h. The dielectric constant tends to relax towards the equilibrium value at each temperature with characteristic time τ. The relaxation seems to proceed with exponential behaviour. The solid line drawn in each figure was determined by fitting the data with the following function:

$$\varepsilon_{\infty 1}(t) = \mathrm{A} \exp(-t/\tau) + \mathrm{B}, \qquad (6)$$

where A and B are constants and t the time. The relaxation times thus derived agree well with the calorimetrically determined data within their experimental errors. Thus the time-dependent behaviour of $\varepsilon_{\infty 1}$ can be correlated with the proton configurational change in the host lattice. The value $\varepsilon_{\infty 1}$ corresponds to the low-frequency limiting value ε_{02} of the permittivity due to the guest polarization. The value ε_{02} decreases as the proton short-range ordering progresses, and increases as the disorder progresses. Thus the coupling between the host and guest dipoles is clearly observed in the short-range ordered state of the host cage.

It is noteworthy that curves A and D observed at

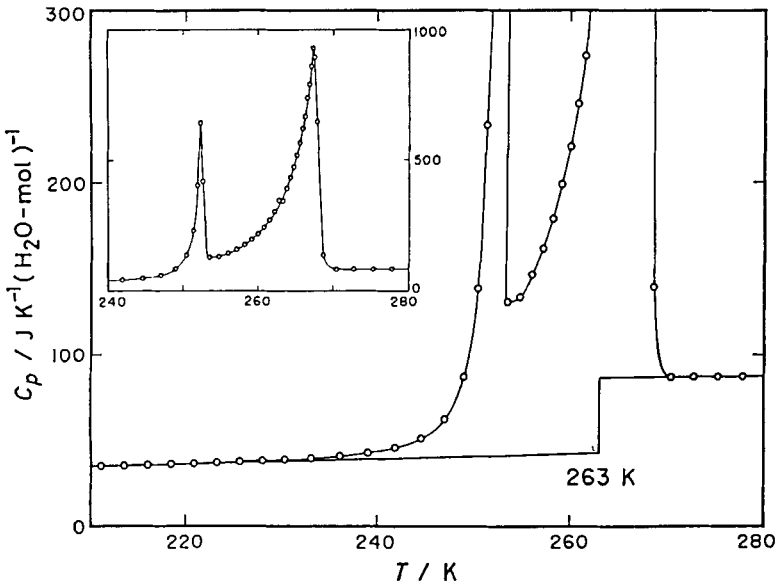

Figure 13 Molar heat capacity of KOH-doped Ac·17H_2O around the incongruent melting point.

the same temperature have different relaxation times. The only difference in the two experiments is the sign and magnitude of the initial departures from the same equilibrium value. Thus the relaxation process is of non-linear nature, which is one of the current topics in the relaxation processes of many glass-forming liquids around their glass transition region. The Kohlrausch–Williams–Watts equation, which allows distribution of the relaxation times, would be a better equation for the reproduction of the experimental data.

Table 1 Thermochemical cycle for the direct determination of the enthalpy of enclathration of acetone(g) into crystalline ice (cr)

Reaction	T(K)	ΔH (kJ)
Ac·16.97H_2O (cr) → Ac·16.97H_2O(l)	263.00	85.3
Ac·16.97H_2O (cr) → Ac·16.97H_2O(l)	273.15	93.0
Ac·16.97H_2O (cr) → 16.97H_2O(l) + Ac(l)	273.15	101.7
Ac·16.97H_2O (cr) → 16.97H_2O(l) + Ac(g)	273.15	134.0
Ac·16.97H_2O (cr) → 16.97H_2O(cr) + Ac(g)	273.15	32.0

Enthalpy of enclathration

Figure 13 gives the heat capacity of the doped Ac hydrate around the melting region. The sharp peak observed at 252.5 K is due to the peritectic point at which the clathrate hydrate decomposes into ice and acetone solution. The separated ice dissolves progressively into the solution with increasing temperature. The process continues further until the next heat-capacity peak is attained at which the solution recovers the original composition. In order to convert the apparent heat capacity and enthalpy change experimentally obtained into the corresponding molar quantities, it is necessary to have many calculations for correction of a minor part of unreacted components. The calculations require some assumptions and lengthy explanation, so that the detailed descriptions are given in a separate paper.[31]

For determination of the enthalpy of fusion, base lines for the crystal and liquid phases were determined. Both heat capacity data for crystal and liquid below and above the melting region were extrapolated simply to a temperature at which the enthalpy change associated with the decomposition and the subsequent dissolution processes become half of the total change. This was determined to be 263 K for the Ac hydrate. For the THF hydrate which exhibits a congruent melting behaviour, the procedure is much more straightforward because of the single step from the crystal to the liquid.[13] Table 1 summarizes the enthalpy change associated with each thermochemical step for the determination of the enthalpy of enclathration of acetone (g) into ice (cr). Literature values of the enthalpy of fusion and vaporization[32] of acetone, the enthalpy of mixing[33] of the acetone-water binary system, and the enthalpy of fusion[16] of ice were used. This is the first successful case of direct determination of the enthalpy of enclathration for the clathrate hydrate possessing an incongruent melting. The value 32.0 kJ mol^{-1} can be compared with the corresponding literature values; 32 kJ mol^{-1} for propylene oxide,[34] 33 kJ mol^{-1} for 1,3-dioxane,[34] and 38 kJ mol^{-1} for 1,3-dioxolane.[34]

Since the frozen-in disordered states of some clathrate hydrates were released by the catalytic action of a minute amount of KOH dopant, it became

possible to determine the absolute entropy of the clathrate hydrate at some reference temperature, say 273.15 K. This value can be combined to those of the component crystals to derive the entropy of enclathration. Thus the combination of the data leads to direct determination of the corresponding Gibbs free energy change, which provides a good basis for comparison with other theoretical approaches to give a better picture of the enclathration process.

Preliminary results of neutron diffraction

Powder diffraction experiments for KOH-doped THF-d_8·17D_2O were performed at 80 K (high temperature phase) and 5 K (low temperature phase). The experimental data and the details for the analysis will be published elsewhere.[35]

The high temperature data were fully analysed by using the Rietveld technique.[36] The space group (Fd3m) and the basic structure of the host lattice determined by Mak and McMullan[37] were used as the starting point of the least-squares fitting. The five-membered ring of the THF molecules was assumed to be a rigid plane. The best model, providing the lowest R factor, is such that the deuterium atom of the water molecule is located with equal probability at the two sites of each hydrogen bond, and the oxygen atom of the THF molecule is pointing to the $\langle 001 \rangle$ axes with its facing molecular plane parallel to the $\{110\}$ planes. There are six equivalent orientations of the THF molecule. Figure 14 shows a schematic drawing of the hexakaidecahedral cage and the enclathrated THF molecule taking in of the six equivalent orientations. The oxygen atoms of the water and THF molecules are represented by open circles and a double circle, respectively, and the carbon atoms by the shaded circles. All of the deuterium atoms are omitted for the sake of clarity. There are four tetrahedrally-located six-membered rings in the cage. The six equivalent orientations are such that the oxygen atom of the THF molecule is pointing to the centre of the bond linking the two six-membered rings, as shown by the closed circles and broken-and-dotted lines in the Figure.

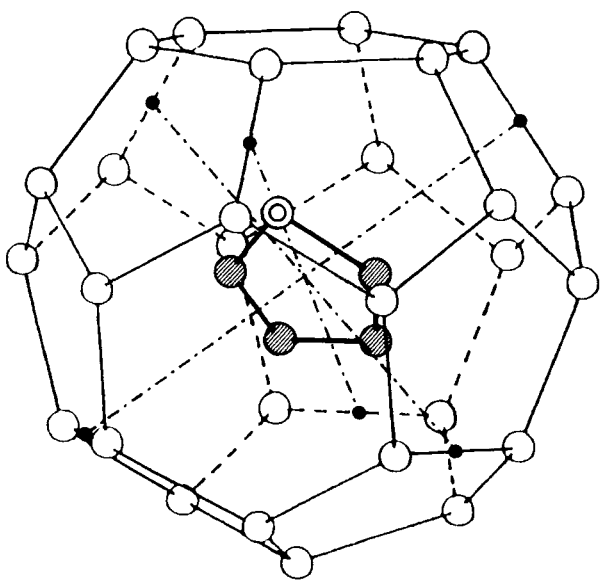

Figure 14 Schematic drawing of the hexakaidecahedral cage of structure II clathrate hydrate and the enclathrated THF molecule in one of the six equivalent orientations. The oxygen atoms of water and THF molecules are represented by open circles and a double circle, respectively, and the carbon atoms by the shaded circles. All of the deuterium atoms are omitted for the sake of clarity. See text for further details.

Analysis of the low temperature phase is not complete because of an unexpected broadening of the diffraction peaks. This is probably due to distortion of the lattice and/or the effect of a small amount of unreacted ice. From the systematic pattern of splitting of the diffraction peaks, the low temperature phase is expected to have an orthorhombic or monoclinic structure which is very similar to tetragonal one (a = 16.96 Å, c = 17.36 Å).

ACKNOWLEDGMENT

The authors would like to express their hearty thanks to the collaborators who have been engaged in the experiments. Financial support from our Ministry of Education through the Grand-in-Aid, the Nissan Science Foundation, the Takeda Science Foundation and the British Council, is gratefully acknowledged.

REFERENCES

1. Powell, H.M.; *J. Chem. Soc. (London)* **1948**, 61.
2. Jeffrey, G.A.; Macmillan, R.K.; *Progr. Inorg. Chem.* **1967**, *8*, 43.
3. Davidson, D.W.; in *Water – A Comprehensive Treatise*, Vol. 2, Franks, F. (Ed), Plenum Press, New York, p. 115.
4. Wilson, G.J.; Davidson, D.W.; *Can. J. Chem.* **1963**, *41*, 264.
5. Rosso, J.-C.; Carbonnel, L.; *Compt. Rend. Acad. Sci. Paris* **1972**, *274C*, 1108.
6. Callanan, J.E.; Sloan, E.D.; *Intl. Gas Res. Conf.* **1983**, 1012.
7. Moriya, K.; Matsuo, T.; Suga, H.; *J. Chem. Thermodyn.* **1982**, *14*, 1143.
8. Matsuo, T.; Suga, H.; *Solid State Commun.* **1977**, *21*, 923.
9. Kuratomi, N.; Yamamuro, O.; Matsuo, T.; Suga, H.; *J. Chem. Thermodym.* **1991**, *23*, 485.
10. Brawer, S.; *Relaxation in Viscous Liquids and Glasses*, American Ceramic Society, Columbus, **1985**.
11. Williams, G.; Watts, D.C.; *Trans. Faraday Soc.* **1970**, *66*, 80.
12. Matsuo, T.; Kishimoto, I.; Suga, H.; Luty, F.; *Solid State Commun.* **1986**, *68*, 177.
13. Yamamuro, O.; Oguni, M.; Matsuo, T.; Suga, H.; *J. Phys. Chem. Solids* **1988**, *49*, 425.
14. Gough, S.R.; Hawkins, R.E.; Morris, B.; Davidson, D.W.; *J. Phys. Chem.* **1973**, *77*, 2969.
15. Hawkins, R.E.; Davidson, D.W.; *J. Phys. Chem.* **1966**, *70*, 1889.

16. Haida, O.; Matsuo, T.; Suga, H.; Seki, S.; *J. Chem. Thermodyn.* **1974**, *6*, 815.
17. Elliott, S.R.; *Physics of Amorphous Materials*, Longman, London, **1984**.
18. Suga, H.; Seki, S.; *J. Non-cryst. Solids* **1974**, *16*, 171.
19. Suga, H.; *Ann. N. Y. Acad. Sci.* **1986**, *484*, 248.
20. Yamamuro, O.p; Kuratomi, N.; Matsuo, T.; Suga, H.; *Solid State Commun.* **1990**, *73*, 317.
21. Yamamuro, O.; Oguni, M.; Matsuo, T.; Sutga, H.; *Solid State Commun.* **1987**, *62*, 289.
22. Kuratomi, N.; Yamamuro, O.; Matsuo, T.; Suga, H.; *J. Therm. Anal.* **1992**, *38*, 1921.
23. Yamamuro, O.; Kuratomi, N.; Matsuo, T.; Suga, H.; *J. Phys. Chem. Solids*, in press.
24. Yamamuro, O.; Suga, H.; *J. Therm. Anal.* **1989**, *35*, 2025.
25. Yamamuro, O.; Matsuo, T.; Suga, H.; *J. Incl. Phenom.* **1990**, *8*, 33.
26. Suga, H.; Matsuo, T.; Yamamuro, O.; *Pure Appl. Chem.* **1992**, *64*, 17.
27. Eisenberg, D.; Kauzmann, W.; *The Structure and Properties of Water*, Clarenden Press, Oxford, **1969**.
28. Bjerrum, N.; *Science* **1951**, *115*, 385.
29. Suga, H.; Matsuo, T.; *Pure Appl. Chem.* **1989**, *61*, 1123.
30. Garg, S.K.; Morris, B.; Davison, D.W.; *J. Chem. Soc., Faraday Trans. II* **1982**, *68*, 481.
31. Kuratomi, N.; Yamamuro, O.; Matsuo, T.; Suga, H.; to be published.
32. Pennington, R.E.; Kobe, K.A.; *J. Am. Chem. Soc.* **1957**, *79*, 300.
33. Kister, A.T.; Waldman, D.C.; *J. Phys. Chem.* **1958**, *62*, 245.
34. Handa, Y.P.; *J. Chem. Thermodyn.* **1985**, *17*, 201.
35. Yamamuro, O.; Matsuo, T.; Suga, H.; David, W.I.F.; Ibberson, R.M.; Leadbetter, A.J.; to be published.
36. Rietveld, H.M.; *J. Appl. Cryst.* **1969**, *2*, 65.
37. Mak, T.C.W.; McMullan, R.K.; *J. Chem. Phys.* **1965**, *42*, 2732.